Tetrahedron 64 (2008) 5208–5216

Contents lists available at ScienceDirect

Tetrahedron

journal homepage: www.elsevier.com/locate/tet

N-Trifyl substituted 1,4-diheterocyclohexanes—stereodynamics and the Perlin effect

Bagrat A. Shainyan [a,*], Igor A. Ushakov [a], Ljudmila L. Tolstikova [a], Andreas Koch [b], Erich Kleinpeter [b,*]

[a] *Irkutsk Institute of Chemistry Siberian Division of Russian Academy of Sciences, 1 Favorsky Street 664033, Irkutsk, Russia*
[b] *Chemisches Institut der Universität Potsdam, PO Box 69 15 53, D-14415 Potsdam, Germany*

ARTICLE INFO

Article history:
Received 29 November 2007
Received in revised form 23 February 2008
Accepted 13 March 2008
Available online 15 March 2008

Keywords:
N-Trifluoromethylsulfonyl derivatives of azinanes
Conformation
Dynamic NMR
Perlin effect
DFT calculations

ABSTRACT

The stereodynamic behaviour of 1-(trifluoromethylsulfonyl)piperidine **1**, 4-(trifluoromethylsulfonyl) morpholine **2**, 1,4-bis(trifluoromethylsulfonyl)piperazine **3** and 4-(trifluoromethylsulfonyl)thiomorpholine 1,1-dioxide **4** was studied by low-temperature ^{1}H, ^{13}C and ^{19}F NMR spectroscopies. In acetone solution, compounds **1**, **2** and **4** were found to exist as mixtures of two conformers in the ratio of 4:1, 4:1 and 8:1, respectively, differing by orientation of the CF_3 group with respect to the ring. Compound **3** exists as a mixture of three conformers in the ratio of 3:28:69 also differing by the orientation of the two CF_3 groups. Unlike the previously studied *N*-trifyl substituted 1,3,5-triheterocyclohexanes, the preferred conformers of compound **1** and of 1,4-diheterocyclohexanes **2**–**4** are those with the CF_3 group directed outward from the ring, which is caused by intramolecular interactions of the oxygen atoms of the CF_3SO_2N groups with the equatorial hydrogens in the α-position. B3LYP/6-311+G(d,p) calculations of the energy, geometry and NMR parameters corroborate the experimental data. The calculated Perlin effects for all conformers of compounds **1**–**4** as well as those measured for the major conformers of compounds **3** and **4** were analyzed by the use of the NBO analysis.

1. Introduction

Conformational behaviour of nitrogen-containing cyclohexanes was the subject of numerous studies summarized in a recent review by one of us.[1] The saturated six-membered ring normally adopts the chair conformation and the substituents occupy the sterically more favourable equatorial position, though in the absence of repulsive interactions one of the substituents at the nitrogen atom(s) may be axial, as in 1,3-dialkyl-1,3-diazinanes and 1,3,5-trialkyl-1,3,5-triazinanes.[2–4] Recently, we have studied the stereodynamics of 5-trifluoromethylsulfonyl-1,3,5-dioxaazinane,[5] 3,5-bis(trifluoromethylsulfonyl)-1,3,5-oxadiazinane,[6] 1,3,5-tris(trifluoromethylsulfonyl)-1,3,5-triazinane,[6,7] and 1-(methylsulfonyl)-3,5-bis(trifluoromethylsulfonyl)-1,3,5-triazinane[8] by low-temperature ^{1}H, ^{13}C, ^{15}N and ^{19}F NMR spectroscopies and quantum-chemical calculations. To the best of our knowledge, no other reports on the stereodynamics of azinanes with electronegative groups at the nitrogen atom(s) are present in the literature. At the same time, the presence of strong acceptors, like the trifyl group CF_3SO_2, may impart the nitrogen it is attached to, the properties of sp^2 rather than sp^3-hybridized atom. In turn, this may result not only in specific stereochemical behaviour, different from that for *N*-alkyl substituted analogues, but also in specific stereoelectronic effects as was shown for the aforementioned 1,3,5-triheterocyclohexanes studied previously.[5–8]

Thus, in continuation of our studies of *N*-trifluoromethyl substituted perhydroazines,[5–12] in the present communication we have investigated the stereodynamic behaviour of 1-(trifluoromethylsulfonyl)piperidine **1**, 4-(trifluoromethylsulfonyl)morpholine **2**, 1,4-bis(trifluoromethylsulfonyl)piperazine **3**, 4-(trifluoromethylsulfonyl)thiomorpholine 1,1-dioxide **4**, and measured $^{1}J_{CH}$ coupling constants for compounds **3** and **4** in order to prove the Perlin effect in these heterocycles (Scheme 1).

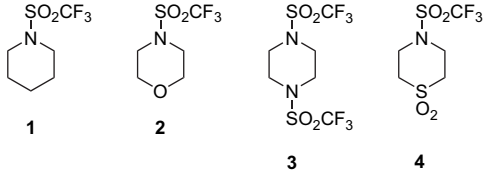

1 **2** **3** **4**

Scheme 1.

* Corresponding authors. Fax: +7 3952 419346 (B.A.S.).
E-mail addresses: bagrat@irioch.irk.ru (B.A. Shainyan), kp@chem.uni-potsdam.de (E. Kleinpeter).

0040-4020/$ – see front matter © 2008 Elsevier Ltd. All rights reserved.
doi:10.1016/j.tet.2008.03.047

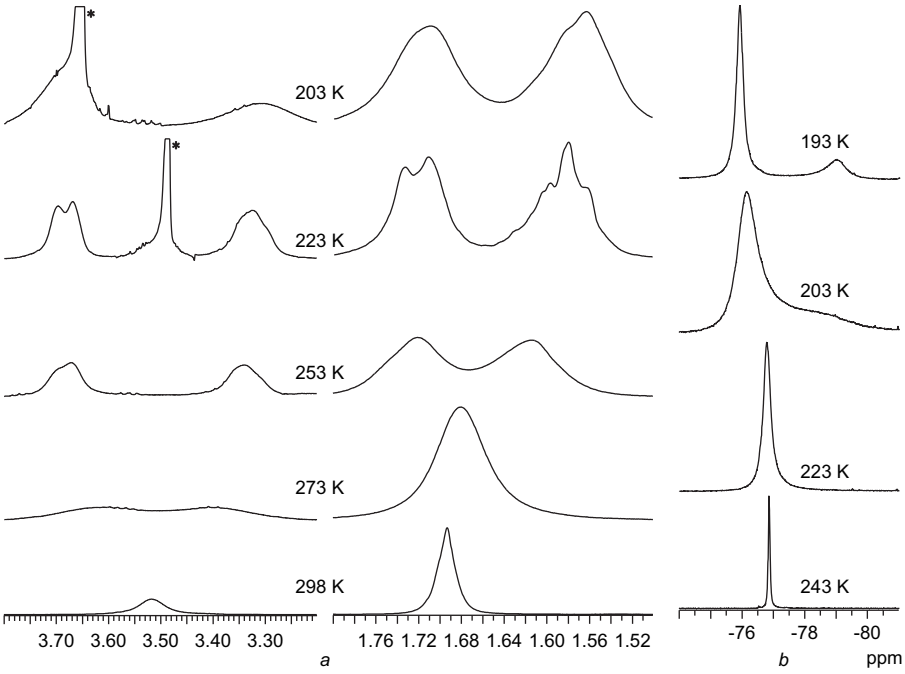

Figure 1. (a) ^{1}H NMR spectra of **1** in acetone-d_6 (asterisk (*) denotes the residual OH signal); (b) ^{19}F NMR spectra of **1** in acetone-d_6.

2. Results and discussion

2.1. 1-(Trifluoromethylsulfonyl)piperidine 1 and 4-(trifluoromethylsulfonyl)morpholine 2

The low-temperature ^{19}F NMR spectra of 1-(trifluoromethylsulfonyl)piperidine **1** and 4-(trifluoromethylsulfonyl)morpholine **2** in acetone solution unambiguously point to the existence of two conformers in the ratio of 4:1 (Figs. 1b and 2b). Taking into account the results of our previous studies of *N*-trifluoromethylsulfonyl derivatives of heterocyclohexanes with the oxygen and/or nitrogen atoms in the 1,3,5-positions,[5–8] these are the conformers differing by the inward or outward orientation of the trifluoromethyl group with respect to the ring (cf. Scheme 2).

The downfield signal in the ^{19}F NMR spectra of **1** and **2** is more intense, similar to previously studied 1,3,5-triheterocyclohexanes.[5–8] However, based on the experimental and computational data, the downfield signal of 1,3,5-triheterocyclohexanes was assigned to the predominant conformer with the inward trifyl group.[5–8] As distinct from that, the B3LYP/6-311+G(d,p) calculations of heterocycles **1** and **2** are indicative of the fact that the conformers with the outward CF_3 group **1b** and **2b** are more stable

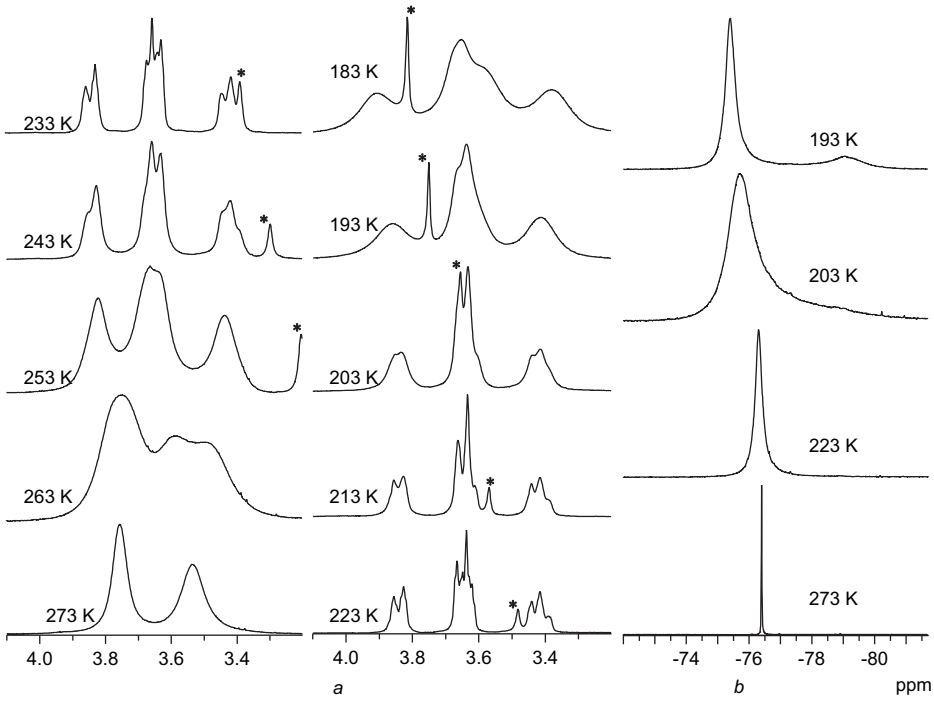

Figure 2. (a) ^{1}H NMR spectra of **2** in acetone-d_6 (asterisk (*) denotes the residual OH signal); (b) ^{19}F NMR spectra of **2** in acetone-d_6.

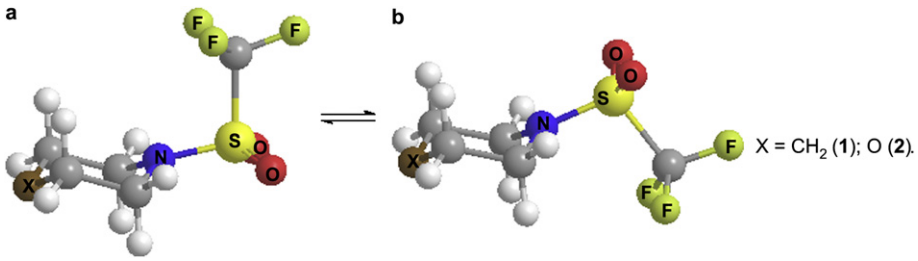

Scheme 2.

than those with the inward CF_3 group **1a** and **2a** by 0.82 and 0.83 kcal mol^{-1}, respectively (see Table SI-1, Supplementary data). The apparent contradiction was removed by calculation of the ^{19}F chemical shifts performed at the GIAO B3LYP/6-311+G(d,p) level. According to these calculations, the ^{19}F signal of the outward CF_3 group is shifted downfield with respect to that of the inward CF_3 group by 5.3 ppm for compound **1** and by 6.0 ppm for compound **2** in good agreement with the experiment (see Table SI-11, Supplementary data).

The energy difference between the 'inward' and the 'outward' conformers of compounds **1** and **2** determined from the experimental ratio of intensities of the signals in the low-temperature ^{19}F NMR spectra, equal to 4:1 (Figs. 1b and 2b), is 0.53 kcal mol^{-1}. The values of $\Delta G^{\#}$(298 K) obtained from the vibrational frequency calculations are equal to 0.22 and 0.60 kcal mol^{-1} for the equilibriums **1a**⇆**1b** and **2a**⇆**2b**, respectively. These data refer to the gas phase; however, since the dipole moments for the 'inward' and the 'outward' conformers of both compounds are virtually equal (see Supplementary data), no significant solvent effect is expected.

At 273 K, the ^{1}H NMR spectrum of 4-(trifluoromethylsulfonyl)-morpholine **2** shows two broadened singlets at 3.55 and 3.75 ppm, which already at 253 K decoalesced to three signals at 3.4, 3.6 and 3.8 ppm due to the frozen six-membered ring interconversion ($\Delta G_c^{\#}$=12.9 kcal mol^{-1}). The signal at 3.4 ppm belongs to the axial protons of the NCH_2 groups, the signal at 3.8 ppm to the equatorial protons of the OCH_2 groups, and the signal at 3.6 ppm is a superposition of the signals of the OCH_2 axial and the NCH_2 equatorial protons. The observed merging of the latter signals is consistent with close values of the calculated chemical shifts of the OCH_{ax} and NCH_{eq} signals: $\delta(OCH_{ax})$=3.60, $\delta(NCH_{eq})$=3.61 ppm for the major conformer **2b**, and $\delta(OCH_{ax})$=3.57, $\delta(NCH_{eq})$=3.42 ppm for the minor conformer **2a** (Table SI-11). Below 203 K, all three signals are broadened, probably due to freezing the restricted rotation about the N–S bond at these temperatures; with the present NMR equipment, the lowest temperature obtained was only 185 K, thus, decoalescence into the rotamers (cf. ^{19}F NMR results—vide supra) actually could not be reached.

2.2. 1,4-Bis(trifluoromethylsulfonyl)piperazine 3

For 1,4-bis(trifluoromethylsulfonyl)piperazine **3** three conformers are possible differing by rotation of the CF_3 groups about the two N–S bonds (cf. Scheme 3).

All three conformers correspond to minima on the potential energy surface, the conformer **3c** being the most stable one, and conformers **3a** and **3b** lying higher in energy by 1.65 and 0.90 kcal mol^{-1}, respectively.

The dynamic exchange phenomena in the ^{1}H and ^{19}F NMR spectra of compound **3** (Fig. 3) are indicative of the existence of an equilibrium between these conformers as a result of two dynamic processes, the ring inversion and rotation about the N–S bond. The interconversion of the corresponding conformers **3a**, **3b** and **3c** is represented in Scheme 4.

At room temperature, the ^{1}H NMR spectrum of compound **3** shows a broadened singlet at 3.8 ppm, which upon cooling to 253 K decoalesce to give three signals at 3.6, 3.8 and 4.0 ppm. The signals at 3.6 and 4.0 ppm belong to the axial and equatorial protons in the most stable conformer **3c**, respectively, whereas the broadened singlet at 3.8 ppm is a result of merging of the signals of all protons of conformer **3b** averaged due to fast ring inversion. Upon further temperature decrease, the ring inversion of conformer **3b** becomes slow (on the NMR scale), the intensity of the signal at 3.8 ppm decreases and at 193 K, it disappears due to decoalescence, the appearing signals of the axial and equatorial protons of conformer **3b** being superimposed with the signals of the corresponding protons of conformer **3c**. Such overlapping results in disappearance of the signals at 3.6 and 4.0 ppm at 203 and 193 K, and at 183 K a visible broadening of the 'basements' of these signals is observed. The conclusions made are confirmed by calculations: the calculated chemical shifts of the axial and equatorial protons in conformer **3b** (3.07 and 3.72 ppm, respectively, at the α-position to the inward CF_3, and 3.02 and 3.83 ppm at the α-position to the outward CF_3) are very close to those of conformer **3c** (3.06 and 3.87 ppm, respectively), the equatorial protons resonating in a lower field.

Though the signals of the minor conformer **3a** in the ^{1}H NMR spectrum could not be seen separately, the existence of all three

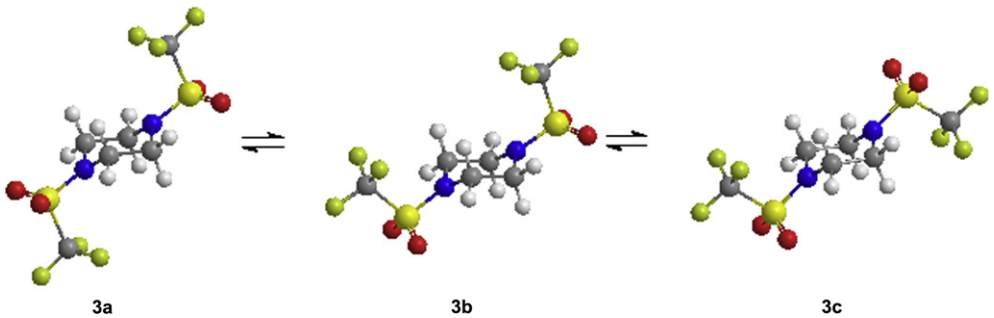

Scheme 3.

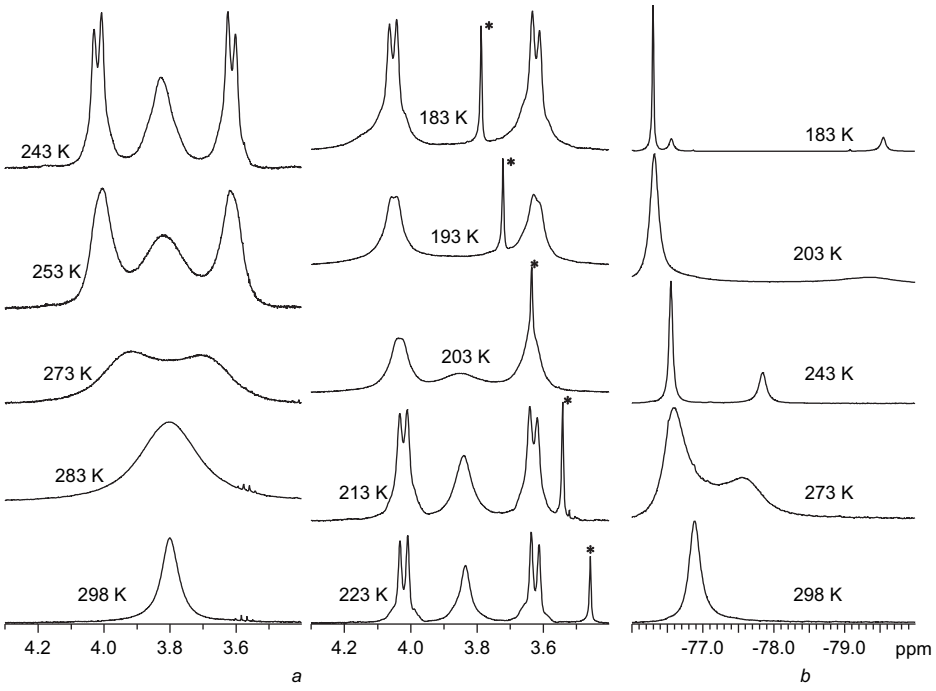

Figure 3. (a) ^{1}H NMR spectra of **3** in acetone-d_6 (asterisk (*) denotes the residual OH signal); (b) ^{19}F NMR spectra of **3** in acetone-d_6.

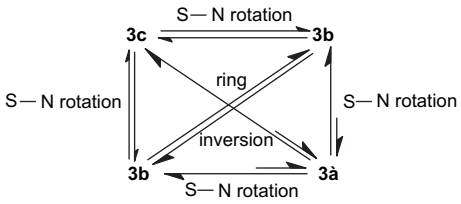

Scheme 4.

conformers of compound **3** in the acetone-d_6 solution is proved by its ^{19}F NMR spectrum at 183 K (Fig. 3b). The intense downfield signal at −76.30 ppm belongs to the two CF_3 groups in conformer **3c**. The signals at −76.56 ppm and −79.56 ppm belong to the outward and the inward CF_3 groups in conformer **3b**, respectively. The presence of the third conformer **3a** is witnessed by different intensity of the signals at −76.56 and −79.56 ppm: the upfield signal is by 23% more intense than the downfield one, due to superposition of the signals of the inward CF_3 group of conformer **3b** and of the two equivalent inward CF_3 groups of conformer **3a**. The ratio of conformers **3a**/**3b**/**3c** at 183 K is 3:28:69, in good correlation with their relative energies (Table SI-1).

2.3. 4-(Trifluoromethylsulfonyl)thiomorpholine 1,1-dioxide 4

In the ^{1}H NMR spectrum of 4-(trifluoromethylsulfonyl)-thiomorpholine 1,1-dioxide **4** at 273 K different signals of NCH_2 and SCH_2 groups at 4.1 and 3.4 ppm, respectively, are observed. The low-temperature ^{1}H and ^{19}F NMR spectra of compound **4** point to the existence of two conformers in the ratio of 8:1 (Fig. 4). In the ^{1}H NMR spectrum at 183 K a doublet signal of one of the protons of the minor conformer at 4.46 ppm can be clearly seen (Fig. 4a). As for compounds **1**–**3**, the major conformer **4b** also has the CF_3 group outward, showing the downfield signal in the ^{19}F NMR spectrum at −77.6 ppm. In the ^{1}H NMR spectrum at 183 K, the signal of one proton of each group is split into a doublet, whereas the other one is split into a triplet (for the triplet at 3.7 ppm a small additional coupling, with J ~2.5 Hz, is observed). The assignment to axial and equatorial protons was made on the basis of their multiplicity and taking into account the calculated chemical shifts and coupling constants. The splitting into a triplet is due to coincidence of the geminal and one of vicinal coupling constants. Only the $^{3}J_{ax-ax}$ coupling constant can be of the same value as the geminal constant ^{2}J, therefore, the signals at 3.7 and 3.9 ppm were assigned to the axial protons of the SCH_2 and NCH_2 group, respectively, and the signals at 3.4 and 4.4 ppm to the equatorial protons of these groups. If so, the SCH_{eq} proton should resonate at a higher field as compared to SCH_{ax}, whereas the NCH_{eq} proton at a lower field as compared to NCH_{ax}. The calculations completely confirm this conclusion: for the SCH_2 group the difference of the chemical shifts is $\Delta\delta_{calcd}=(\delta_{CHax}-\delta_{CHeq})=(2.85-2.59)=0.26$ ppm ($\Delta\delta_{exp}$ 0.31 ppm), whereas for the NCH_2 group $\Delta\delta_{calcd}=(3.41-3.96)=-0.55$ ppm ($\Delta\delta_{exp}$ −0.49 ppm) (Table SI-11).

The splitting of the signals of equatorial protons of the SCH_2 and NCH_2 groups into doublets, seen in Figure 4, is due to the small vicinal coupling constants $^{3}J_{eq-ax}$ and $^{3}J_{eq-eq}$. According to the theoretical calculations, the coupling constants $^{3}J_{eq-ax}$ and $^{3}J_{eq-eq}$ in the major conformer **4b** are equal to 2.5–4.0 Hz, and the experimental half-width of the SCH_{eq} and NCH_{eq} signals reaches 5.5 Hz. At the same time, the calculated constant $^{3}J_{ax-ax}$ (11.1 Hz) is very close to the geminal constants ^{2}J, 13.0 and 13.3 Hz for the SCH_2 and NCH_2 groups, respectively.

The energy difference of conformers **4a** and **4b** determined experimentally from the ratio of intensities of the signals in the low-temperature ^{1}H and ^{19}F NMR spectra equal to 1:8, is 0.76 kcal mol^{-1} and practically coincides with the calculated value of ΔE (0.82 kcal mol^{-1}). The calculated value of $\Delta G^{\#}$ (298 K) for the equilibrium **4a**⇆**4b** is equal to 1.96 kcal mol^{-1}.

2.4. Relative stability of the ‘inward’ vs ‘outward’ conformers

The principal difference of compounds **1**–**4** studied in this work from the earlier studied 1,3,5-triheterocyclohexanes[5–8] is that the preferred conformers of compounds **1**–**4** have the CF_3 group

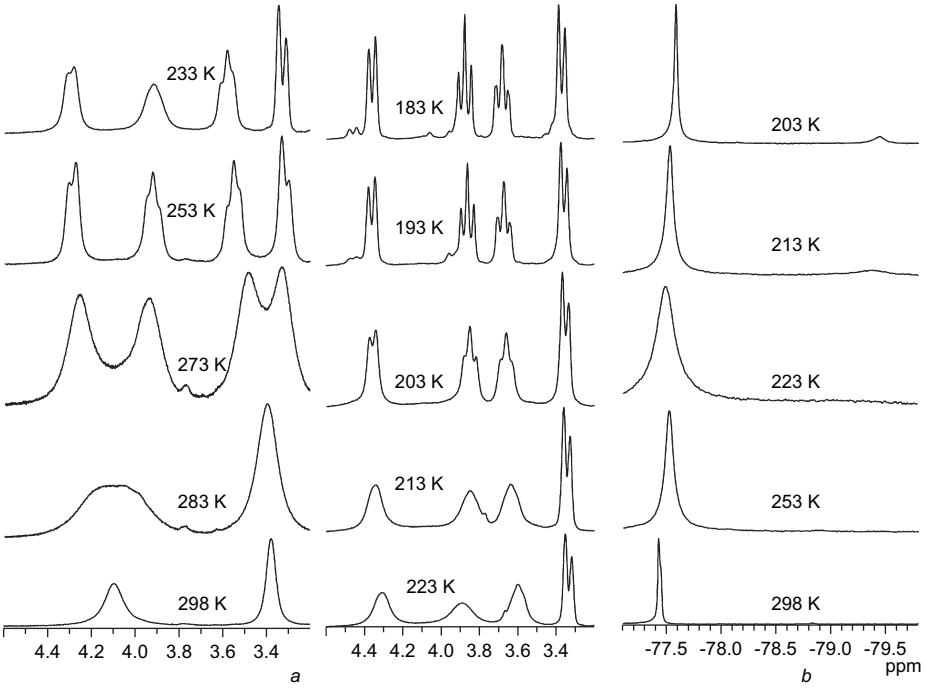

Figure 4. (a) ^{1}H NMR spectra of **4** in acetone-d_6; (b) ^{19}F NMR spectra of **4** in acetone-d_6.

outward, whereas the predominant conformers of 5-trifluoromethylsulfonyl-1,3,5-dioxaazinane,[5] 1,3,5-tris(trifluoromethylsulfonyl)-1,3,5-triazinane,[6,7] 1-methylsulfonyl-3,5-bis(trifluoromethylsulfonyl)-1,3,5-triazinane[8] and 3,5-bis(trifluoromethylsulfonyl)-1,3,5-oxadiazinane[6] have the CF_3 group inward. The structural differences of the 1,4-diheterocyclohexanes studied and the earlier studied 1,3,5-triheterocyclohexanes amount to different directionality of the slightly pronounced nitrogen atom pyramid, as shown below on the example of the calculated geometries of 4-(trifluoromethylsulfonyl)morpholine and 5-trifluoromethylsulfonyl-1,3,5-dioxazinane (cf. Scheme 5). The sum of the bond angles at nitrogen for both types of the heterocycles is only slightly distinct from 360°; for compounds **1**–**4** the calculated deviation is 0.1°–2.3° for the conformers with the CF_3 group outward and 0.1°–5.3° for those with the CF_3 group inward. For the earlier studied 1,3,5-triheterocyclohexanes the deviations are similar.

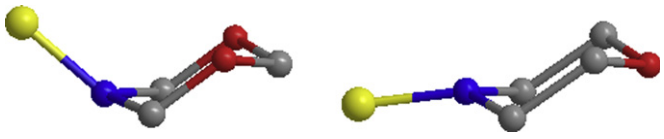

Scheme 5.

However, these seemingly small distinctions schematically depicted in Scheme 5 (with the trifyl group represented as one atom regardless of its conformation) may cause qualitative differences of the relative stability of different conformers for the two types of the heterocycles. We assume that different relative stability of the inward and outward conformers of 1,4-dihetero- and 1,3,5-triheterocyclohexanes is due to intramolecular interactions of the oxygen atoms of the CF_3SO_2N groups with the equatorial hydrogen atoms in the α-position, since only these O···H distances, which in all conformers of all studied compounds equate to ca. 2.4 Å, are less than the sum of the van-der-Waals radii (2.6 Å). The parameter, which is notably distinct for the conformers of the studied compounds with the inward and outward CF_3 group, is the charge on the NSO_2 oxygen atoms. Indices $f=(q_O \cdot q_{Heq})/r_{O\cdots H}$, characterizing the O···H nonvalent interaction are given in Table 1.

As can be clearly seen from Table 1, for all studied 1,4-diheterocyclohexanes **1**–**4** the attractive O···H interaction is stronger in conformers with the CF_3 group outward, whereas for all 1,3,5-triheterocyclohexanes this interaction is stronger in the conformers with the CF_3 group inward in excellent agreement with the results of conformational analysis.

2.5. Perlin effect and NBO analysis

Another interesting point is the Perlin effect in compounds **1**–**4**. According to our previous studies on 1,3,5-triheterocyclohexanes,[5–8] the CH_2 group in the $O_2SNCH_2NSO_2$ fragments shows the reverse Perlin effect ($^{1}J_{CHeq}<{}^{1}J_{CHax}$), whereas the corresponding OCH_2NSO_2 fragments shows the normal Perlin effect ($^{1}J_{CHeq}>{}^{1}J_{CHax}$). That means that hyperconjugation effect $n_O \rightarrow \sigma^*(C–H_{ax})$ predominates overall possible effects of the NSO_2CF_3 or NSO_2CH_3 groups leading to a relative decrease of $^{1}J_{CHeq}$ with respect to $^{1}J_{CHax}$ in the latter compounds. Unfortunately, we were unable to measure the $^{1}J_{CH}$ values for all compounds, but rather only for the major conformers of **3** and **4**. Nevertheless, since calculations at the B3LYP/6-311+G(d,p) level of theory were shown to correctly reproduce at least the sign of the Perlin effect,[5,7] we believe it possible to use for analysis of the Perlin effect in compounds **1**–**4** the calculated values of $\Delta J=({}^{1}J_{CHeq}-{}^{1}J_{CHax})$ the more so that for compounds **3** and **4** they are in good agreement with the experimental ones (Table 2).

The experimental values of $^{1}J_{CH}$ were obtained from cross-sections of the 2D heteronuclear {^{1}H–^{13}C} HSQC spectra recorded without wide band decoupling from ^{13}C by GARP pulse sequence; the digital resolution for the proton channel in the HSQC experiments was 0.2 Hz. As an example, the 2D-HSQC spectrum of 4-(trifluoromethylsulfonyl)thiomorpholine 1,1-dioxide **4** at 183 K is presented in Figure 5.

The Perlin effect and analysis of contributions of various stereoelectronic effects into the value of $^{1}J_{CH}$ were the subject of numerous studies[13–24] as discussed in detail in our previous work.[6]

Table 1
Indices $f=100(q_O \cdot q_{Heq})/r_{O\cdots H}$, where q_O and q_{Heq} are charges on oxygen atoms and equatorial hydrogens in the α-position to nitrogen, $r_{O\cdots H}$ is the distance between the interacting atoms (Å)

Compound	CF_3 inward	CF_3 outward	Lit.
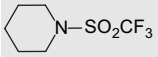	0.95	1.05	This work
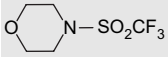	0.82	1.01	This work
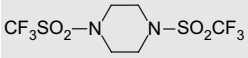	0.66	0.79	This work
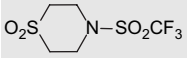	0.70	1.33	This work
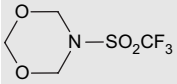	1.25	0.86	12
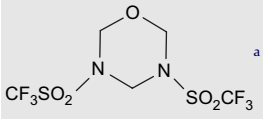 [a]	1.12	0.33	5
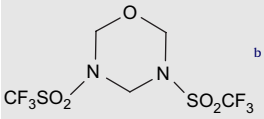 [b]	—	0.42	5
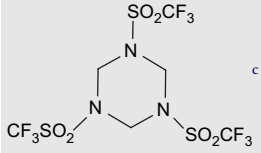 [c]	1.09	0.37	6
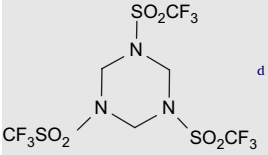 [d]	—	0.11	6
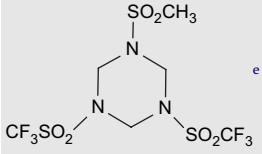 [e]	3.83	3.54	7
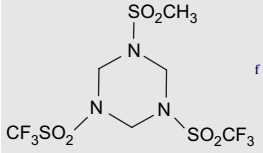 [f]	3.45	3.31	7

[a] One CF_3 group inward, one outward.
[b] Both CF_3 groups outward.
[c] One CF_3 group inward, two outward.
[d] Three CF_3 groups outward.
[e] Me group inward, both CF_3 groups outward; interaction with α-CH_2 group to $MeSO_2$.
[f] One CF_3 group inward, one outward; for CH_2 group in $CF_3SO_2NCH_2NSO_2CF_3$ fragment.

First, it should be noted that the sign of the Perlin effect in compounds **1**–**4** does not depend on the orientation of the CF_3 group, being the same in the major and minor conformers. Second, in all cases, except for the SCH_2 groups in compound **4**, the C–H_{eq} bonds are shorter than the corresponding C–H_{ax} bonds (Table 2). That means that the normal Perlin effect is observed for the 2(6)- and 4-CH_2 groups of compound **1** and for the OCH_2 groups of compound **2**. The SCH_2 groups of compound **4** shows the reverse Perlin effect which, however, falls into the Wolfe's modified definition[13,19a] of the *normal* Perlin effect (the larger $^1J_{CH}$ for the longer C–H bond). In all other cases the Perlin effect should be considered as *genuine reverse*, both in the original and modified definitions. This refers to the 3(5)-CH_2 groups in compound **1**, the NCH_2 groups in compound **2**, all (equivalent) CH_2 groups in compound **3** and the NCH_2 groups in compound **4**. For compounds **3** and **4**, the theoretically calculated reverse Perlin effects were proved experimentally by measuring the $^1J_{CH}$ coupling constants for the major conformers of these compounds (Table 2). For the interpretation of the Perlin effects in compounds **1**–**4** possible orbital interactions in their most stable conformers obtained from the NBO analysis and presented in Table 3 were considered.

For compound **1**, the Perlin effect in the α-position to the nitrogen atom is determined by the balance of the $\sigma(C–H_{ax})\rightarrow\sigma^*(C–H_{ax})$ and $n_N\rightarrow\sigma^*(C–H_{ax})$ interactions leading to the normal Perlin effect, and donation from the $\sigma(C–H_{eq})$ orbital to all appropriate adjacent σ^* orbitals leading to the reverse. The total second order perturbation energy of the former interactions involving the C–H_{ax} bond is 11.4 kcal mol^{-1}, whereas the energy of those involving the C–H_{eq} bond is by 2.5 kcal mol^{-1} less (Table 3). Note that the CH_2 group in the NCH_2N fragments of 1,3,5-triheterocyclohexanes shows the reverse Perlin effect.[6,8] The overall normal calculated Perlin effect for the NCH_2 group in compound **1** (Table 2) is first due to a $n_N\rightarrow\sigma^*(C–H_{ax})$ contribution from the slightly pyramidal nitrogen atom (Σ_N 357.6°), and second, due to interaction of the $\sigma(C–H_{eq})$ orbital with only one σ^*(N–C) orbital and not with two, as in NCH_2N fragments of the previously studied 1,3,5-triheterocyclohexanes.[5–8]

A small reverse Perlin effect for the CH_2 group in the β-position can be rationalized as a result of slight predomination of the $\sigma(C–H_{eq})\rightarrow\sigma^*(C–N)$ hyperconjugation over the $\sigma(C–H_{ax})\rightarrow\sigma^*(C–H_{ax})$ interaction due to a decrease of the σ^*(C–N) orbital energy owing to the presence of a strong acceptor at the nitrogen atom. However, the data of Table 3 predict normal Perlin effect, therefore, other interactions (omitted in Table 3) must be additionally taken into consideration to rationalize the overall effect.

Finally, the normal Perlin effect for the CH_2 group in the γ-position clearly results from the predominating $\sigma(C–H_{ax})\rightarrow\sigma^*(C–H_{ax})$ hyperconjugation (11.0 vs 9.3 kcal mol^{-1}, Table 3).

The normal Perlin effect for the OCH_2 group in compound **2** is mainly the result of classical $n_O\rightarrow\sigma^*(C–H_{ax})$ hyperconjugation, which makes the largest contribution of 6 kcal mol^{-1} (Table 3).

Qualitatively, the observed small reverse Perlin effect for the NCH_2 group in compound **2** is due to predomination of the $\sigma(C–H_{eq})\rightarrow\sigma^*(C–O)$ and $\sigma(C–H_{eq})\rightarrow\sigma^*(C–N)$ interactions over the $n_N\rightarrow\sigma^*(C–H_{ax})$ hyperconjugation. Other orbital interactions (including those omitted in Table 3) counterbalance each other.

Similarly, the experimentally proved reverse Perlin effect for all NCH_2 groups in compound **3** is due to strong orbital interactions $\sigma(C–H_{eq})\rightarrow\sigma^*(C–N)$ and $\sigma(C–H_{eq})\rightarrow\sigma^*(N–S)$ that outweigh the $\sigma(C–H_{ax})\rightarrow\sigma^*(C–H_{ax})$ and $n_N\rightarrow\sigma^*(C–H_{ax})$ interactions (Table 3).

For the NCH_2 group in **4**, the orbital interactions involving the C–H_{ax} and the C–H_{eq} bonds are counterbalanced within 0.5 kcal mol^{-1}, therefore, no definite conclusion can be made from the NBO analysis regarding the sign of the Perlin effect. For the SCH_2 group in **4**, strong interaction $\sigma(C–H_{eq})\rightarrow\sigma^*(C–N)$ also results in notable predomination of orbital interactions involving the C–H_{eq} bond over those involving the C–H_{ax} bond (8.5 vs 6.9 kcal mol^{-1}, Table 3) in agreement with the largest reverse Perlin effect observed experimentally (Table 2).

Table 2
Calculated bond distances l (Å), coupling constants $^1J_{CH}$ (Hz) and Perlin effect $\Delta J=(^1J_{CHeq}-^1J_{CHax})$ in compounds **1–4**

Conformer	NCH					XCH				
	l_{CHeq}	l_{CHax}	$^1J_{CHeq}$	$^1J_{CHax}$	Perlin effect	l_{CHeq}	l_{CHax}	$^1J_{CHeq}$	$^1J_{CHax}$	Perlin effect
1a[a]	1.088	1.098	136.9	132.3	4.6	1.094	1.095	122.6	124.1	−1.5
1b[b]	1.088	1.098	136.7	131.2	5.5	1.094	1.095	122.7	125.0	−2.3
2a	1.090	1.097	135.1	136.8	−1.7	1.092	1.100	139.9	136.1	3.8
2b	1.090	1.097	135.1	135.5	−0.4	1.092	1.100	139.9	137.0	2.9
3a	1.089	1.096	136.2	138.0	−1.8	1.089	1.096	136.2	138.0	−1.8
3b	1.089	1.096	136.2	138.9	−2.7	1.089	1.096	136.2	138.9	−2.7
3c	1.089	1.096	136.1 (144.8)	137.9 (148.4)	−1.8 (−3.6)	1.089	1.096	136.1 (144.8)	137.9 (148.4)	−1.8 (−3.6)
4a	1.089	1.094	138.2	141.4	−3.2	1.092	1.091	136.2	139.4	−3.2
4b	1.089	1.093	137.6 (145.1)	141.0 (148.8)	−3.4 (−3.7)	1.092	1.091	136.3 (137.5)	140.4 (143.6)	−4.1 (−6.1)

Experimental values are given in brackets.
[a] For 4-CH_2 group l_{CHeq} 1.094 Å, J_{CHeq} 125.0 Hz, l_{CHax} 1.098 Å, J_{CHax} 119.7 Hz.
[b] For 4-CH_2 group l_{CHeq} 1.094 Å, J_{CHeq} 125.2 Hz, l_{CHax} 1.098 Å, J_{CHax} 119.4 Hz.

3. Conclusions

Multinuclear low-temperature NMR of *N*-trifyl substituted 1,4-diheterocyclohexanes [1-(trifluoromethylsulfonyl)piperidine, 4-(trifluoromethylsulfonyl)morpholine, 1,4-bis(trifluoromethylsulfonyl)piperazine and 4-(trifluoromethylsulfonyl)thiomorpholine 1,1-dioxide] in conjunction with theoretical calculations revealed the existence of the conformers with different orientation of the CF_3SO_2 group with respect to the heterocyclic ring. The calculations were immanently important to simulate, visualize or understand the dynamic processes actually taking place. The studied compounds are different from the earlier investigated *N*-trifyl substituted 1,3,5-triheterocyclohexanes in that for the latter the most stable conformers were those with the trifyl group directed inward the ring whereas for the former the outward conformers are preferable. Analysis of our own results and the literature data on the Perlin effect in many heterocyclohexanes suggests that though the effect can be rationalized by considering a balance of various stereoelectronic effects, it is still far from being predictable, except for the simplest cases, like in cyclohexane itself, pyrans, or 1,3-dioxanes.

4. Experimental section

4.1. General

Synthesis, physico-chemical characteristics, and the ^1H, ^{13}C, ^{15}N and ^{19}F NMR spectra for compounds **1–4** are described in our previous work.[12]

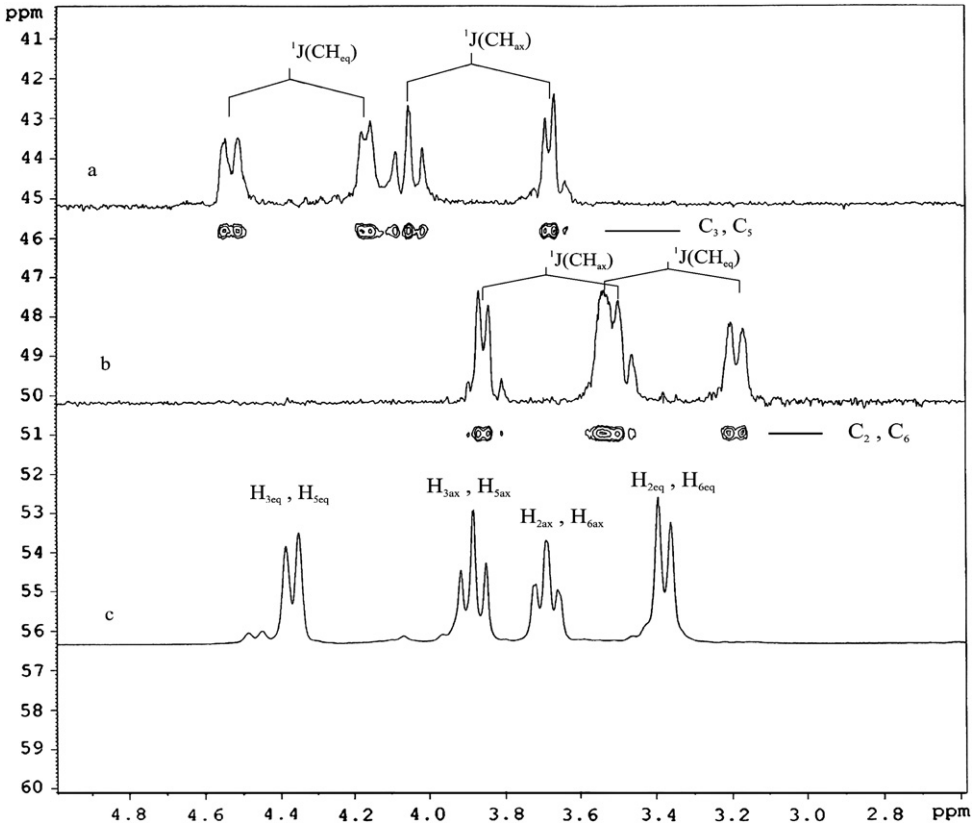

Figure 5. 2D-HSQC spectrum of compound **4** at 183 K. (a) Cross-section of the spectrum at the resonance frequency of C3(5); (b) Cross-section of the spectrum at the resonance frequency of C2(6); (c) ^1H NMR spectrum.

Table 3
Second order perturbation energies (kcal mol^{-1}) for orbital interactions of the C–H bonds in 1-(trifluoromethylsulfonyl)piperidine **1b**, 1-(trifluoromethylsulfonyl)morpholine **2b**, 1,4-bis(trifluoromethylsulfonyl)piperazine **3c** and 4-(trifluoromethylsulfonyl)thiomorpholine 1,1-dioxide **4b** from NBO calculations

1b		**2b**		**3c**		**4b**	
$\sigma(NC–H_{ax})\rightarrow\sigma^*(C–H_{ax})$	2.46	$\sigma(OC–H_{ax})\rightarrow\sigma^*(NC–H_{ax})$	2.53	$\sigma(C–H_{ax})\rightarrow\sigma^*(N–S)$	0.83	$\sigma(NC–H_{ax})\rightarrow\sigma^*(N–S)$	2.48
$\sigma(C–H_{ax})\rightarrow\sigma^*(NC–H_{ax})$	2.77	$\sigma(NC–H_{ax})\rightarrow\sigma^*(OC–H_{ax})$	2.28	$\sigma(C–H_{ax})\rightarrow\sigma^*(C–H_{ax})$	2.36	$\sigma(NC–H_{ax})\rightarrow\sigma^*(SC–H_{ax})$	2.62
$n(N)\rightarrow\sigma^*(C–H_{ax})$	6.17	$n_1(O)\rightarrow\sigma^*(C–H_{ax})$	0.74	$n(N)\rightarrow\sigma^*(C–H_{ax})$	6.20	$\sigma(SC–H_{ax})\rightarrow\sigma^*(NC–H_{ax})$	2.28
$\sigma(C–H_{eq})\rightarrow\sigma^*(N–C)$	3.93	$n_2(O)\rightarrow\sigma^*(C–H_{ax})$	6.01	$\sigma(C–C)\rightarrow\sigma^*(C–H_{eq})$	0.56	$n(N)\rightarrow\sigma^*(C–H_{ax})$	4.63
$\sigma(C–H_{eq})\rightarrow\sigma^*(C–C)$	2.65	$\sigma(OC–H_{eq})\rightarrow\sigma^*(N–C)$	3.28	$\sigma(C–H_{eq})\rightarrow\sigma^*(N–C)$	3.89	$\sigma(OC–H_{eq})\rightarrow\sigma^*(N–C)$	4.05
$\sigma(N–C)\rightarrow\sigma^*(C–H_{eq})$	0.77	$\sigma(OC–H_{eq})\rightarrow\sigma^*(O–C)$	3.08	$\sigma(C–H_{eq})\rightarrow\sigma^*(C–N)$	3.28	$\sigma(OC–H_{eq})\rightarrow\sigma^*(C–S)$	3.67
$\sigma(C–C)\rightarrow\sigma^*(C–H_{eq})$	1.57	$\sigma(N–C)\rightarrow\sigma^*(OC–H_{eq})$	0.93	$\sigma(N–C)\rightarrow\sigma^*(C–H_{eq})$	0.83	$\sigma(N–C)\rightarrow\sigma^*(OC–H_{eq})$	0.74
$\sigma(C_\beta–H_{ax})\rightarrow\sigma^*(C_\alpha–H_{ax})$	2.76	$\sigma(O–C)\rightarrow\sigma^*(OC–H_{eq})$	1.00	$\sigma(C–N)\rightarrow\sigma^*(C–H_{eq})$	0.97	$\sigma(S–C)\rightarrow\sigma^*(OC–H_{eq})$	1.90
$\sigma(C_\beta–H_{ax})\rightarrow\sigma^*(C_\gamma–H_{ax})$	2.74	$n_1(O)\rightarrow\sigma^*(C–H_{eq})$	2.55	$\sigma(N–S)\rightarrow\sigma^*(C–H_{eq})$	0.80	$\sigma(S–N)\rightarrow\sigma^*(OC–H_{eq})$	1.11
$\sigma(C_\alpha–H_{ax})\rightarrow\sigma^*(C_\beta–H_{ax})$	2.45	$\sigma(NC–H_{ax})\rightarrow\sigma^*(N–S)$	0.66			$\sigma(SC–H_{ax})\rightarrow\sigma^*(S–O)$	1.76
$\sigma(C_\gamma–H_{ax})\rightarrow\sigma^*(C_\beta–H_{ax})$	2.77	$\sigma(OC–H_{ax})\rightarrow\sigma^*(NC–H_{ax})$	2.53			$\sigma(S–O1)\rightarrow\sigma^*(SC–H_{ax})$	0.69
$\sigma(C_\beta–H_{eq})\rightarrow\sigma^*(N–C)$	3.78	$n(N)\rightarrow\sigma^*(C–H_{ax})$	6.38			$\sigma(S–O2)\rightarrow\sigma^*(SC–H_{ax})$	1.23
$\sigma(C_\beta–H_{eq})\rightarrow\sigma^*(C–C)$	2.81	$\sigma(C–H_{eq})\rightarrow\sigma^*(N–C)$	3.77			$\sigma(N–C)\rightarrow\sigma^*(SC–H_{eq})$	0.97
$\sigma(N–C)\rightarrow\sigma^*(C_\beta–H_{eq})$	1.02	$\sigma(C–H_{eq})\rightarrow\sigma^*(O–C)$	3.60			$\sigma(C–C)\rightarrow\sigma^*(C–H_{eq})$	0.52
$\sigma(C–C)\rightarrow\sigma^*(C_\beta–H_{eq})$	1.76	$\sigma(O–C)\rightarrow\sigma^*(C–H_{eq})$	0.94			$\sigma(C–H_{eq})\rightarrow\sigma^*(N–C)$	3.57
$\sigma(C–C)\rightarrow\sigma^*(C_\gamma–H_{eq})$	1.63	$\sigma(N–C)\rightarrow\sigma^*(C–H_{eq})$	0.83			$\sigma(C–H_{eq})\rightarrow\sigma^*(S–C)$	1.23
$\sigma(C_\gamma–H_{eq})\rightarrow\sigma^*(C–C)$	3.00	$\sigma(N–S)\rightarrow\sigma^*(C–H_{eq})$	0.71			$\sigma(S–C)\rightarrow\sigma^*(C–H_{eq})$	1.06
		$n_2(O)\rightarrow\sigma^*(C–H_{eq})$	0.61			$\sigma(S–O)\rightarrow\sigma^*(C–H_{eq})$	0.55
						$n(N)\rightarrow\sigma^*(C–H_{eq})$	0.64

4.2. NMR measurements

Dynamic ^{1}H, ^{13}C and ^{19}F NMR spectra were recorded in acetone-d_6 at working frequencies 400 (^{1}H), 100 (^{13}C) and 376 (^{19}F) MHz; ^{1}H and ^{13}C NMR chemical shifts are reported in parts per million downfield to TMS and ^{19}F NMR in parts per million downfield to $CFCl_3$. The temperature was varied by the use of a variable temperature unit, temperature stability of $\pm0.2^\circ$.

4.3. Theoretical calculations

All calculations were performed using the Gaussian 03 suite of programs.[25] Energy calculations with full optimization of all variables as well as calculations of vibrational frequencies and thermodynamic parameters were performed at the B3LYP/6-311+G(d,p) level of theory with the basis set augmented with polarization functions on heavy atoms. The zero point vibrational energies were not scaled for the calculations of the relative thermodynamic parameters. NMR computations of absolute shieldings and spin–spin coupling constants were performed using the GIAO method[26,27] at the same level of theory. The ^{1}H and ^{19}F chemical shifts were calculated using the corresponding absolute shieldings calculated for Me_4Si and $CFCl_3$ at the same level of theory and are given in Table SI-11, Supplementary data. The NBO analysis[28] as implemented in the Gaussian 03 package, was performed for the most stable conformers of molecules **1**–**4**.

Acknowledgements

The financial support of this work by the Russian Foundation for Basic Research (Grant No. 07-03-00425) and Deutsche Forschungsgemeinschaft (Grant RFBR-DFG No. 07-03-91559) is acknowledged.

Supplementary data

Supplementary data include the energy and geometry for the conformers of compounds **1**–**4** and the results of NBO analysis at the B3LYP/6-311+G(d,p) level of theory. Supplementary data associated with this article can be found in the online version, at doi:10.1016/j.tet.2008.03.047.

References and notes

1. Kleinpeter, E. *Adv. Heterocycl. Chem.* **2004**, *86*, 41–127.
2. Jewett, J. G.; Breeyear, J. J.; Brown, J. H.; Bushweller, C. H. *J. Am. Chem. Soc.* **2000**, *122*, 308–323.
3. Anderson, J. E.; Casarini, D.; Ijeh, A. I.; Lunazzi, L.; Tocher, D. A. *J. Am. Chem. Soc.* **1995**, *117*, 3054–3056.
4. dos Santos, F. P.; Tormena, C. F. *J. Mol. Struct. THEOCHEM.* **2006**, *763*, 145–148.
5. (a) Sigalov, M. V.; Shainyan, B. A.; Meshcheryakov, V. I.; Moskalik, M. Y. *Book of Abstracts of 15th European Symposium Fluorine Chemistry*, Prague, Czech Republic, July 15–20, 2007; p 249; (b) Shainyan, B. A.; Ushakov, I. A.; Mescheryakov, V. I.; Koch, A.; Kleinpeter, E. *Tetrahedron*. doi:10.1016/j.tet.2008.03.019
6. Shainyan, B. A.; Ushakov, I. A.; Mescheryakov, V. I.; Schilde, U.; Koch, A.; Kleinpeter, E. *Tetrahedron* **2007**, *63*, 11828–11837.
7. Shainyan, B. A.; Mescheryakov, V. I.; Albanov, A. I.; Sigalov, M. V. *Tetrahedron Lett.* **2005**, *46*, 6199–6201.
8. Shainyan, B. A.; Ushakov, I. A.; Koch, A.; Kleinpeter, E. *J. Org. Chem.* **2006**, *71*, 7638–7642.
9. Mescheryakov, V. I.; Albanov, A. I.; Shainyan, B. A. *Russ. J. Org. Chem. (Engl. Transl.)* **2005**, *41*, 1381–1386.
10. Mescheryakov, V. I.; Albanov, A. I.; Shainyan, B. A.; Zavodnik, V. E.; Bel'skii, V. K. *Russ. J. Org. Chem. (Engl. Transl.)* **2006**, *42*, 1254–1255.
11. Mescheryakov, V. I.; Danilevich, Y. S.; Moskalik, M. Y.; Stetsjura, N. Y.; Zavodnik, V. E.; Bel'skii, V. K.; Shainyan, B. A. *Russ. J. Org. Chem. (Engl. Transl.)* **2007**, *43*, 793–800.
12. Shainyan, B. A.; Tolstikova, L. L.; Zhnikin, A. R. *Russ. J. Org. Chem. (Engl. Transl.)* **2003**, *39*, 1180–1182.
13. Perlin, A. S.; Casu, B. *Tetrahedron Lett.* **1969**, *10*, 2921–2924.
14. (a) Wolfe, S.; Pinto, B. M.; Varma, V.; Leung, R. Y. N. *Can. J. Chem.* **1990**, *68*, 1051–1062; (b) Wolfe, S.; Kim, C.-K. *Can. J. Chem.* **1991**, *69*, 1408–1412.
15. Bailey, W. F.; Rivera, A. D.; Rossi, K. *Tetrahedron Lett.* **1988**, *29*, 5621–5624.
16. (a) Juaristi, E.; Cuevas, G. *Tetrahedron* **1992**, *48*, 5019–5087; (b) Juaristi, E.; Cuevas, G. *Tetrahedron Lett.* **1992**, *33*, 1847–1850; (c) Juaristi, E.; Cuevas, G.; Flores-Vela, A. *Tetrahedron Lett.* **1992**, *33*, 6927–6930; (d) Juaristi, E.; Cuevas, G.; Vela, A. *J. Am. Chem. Soc.* **1994**, *116*, 5796–5804; (e) Cuevas, G.; Juaristi, E.; Vela, A. *J. Mol. Struct. THEOCHEM* **1997**, *418*, 231–241; (f) Cuevas, G.; Juaristi, E.; Vela, A. *J. Phys. Chem. A* **1999**, *103*, 932–937; (g) Cuevas, G.; Juaristi, E. *J. Am. Chem. Soc.* **2002**, *124*, 13088–13096; (h) Juaristi, E.; Rosquete-Pina, G. A.; Vásquez-Hernández, M.; Mota, A. J. *Pure Appl. Chem.* **2003**, *75*, 589–599.
17. (a) Anderson, J. E.; Bloodworth, A. J.; Cai, J. Q.; Davies, A. G.; Schiesser, C. H. *J. Chem. Soc., Perkin Trans. 2* **1993**, 601–602; (b) Cai, J. Q.; Davies, A. G.; Schiesser, C. H. *J. Chem. Soc., Perkin Trans. 2* **1994**, 1151–1156; (c) Anderson, J. E.; Bloodworth, A. J.; Cai, J. Q.; Davies, A. G.; Tallant, N. A. *J. Chem. Soc., Chem. Commun.* **1992**, 1689–1690; (d) Anderson, J. E.; Cai, J. Q.; Davies, A. G. *J. Chem. Soc., Perkin Trans. 2* **1997**, 2633–2638.
18. Randell, K. D.; Johnston, B. D.; Green, D. F.; Pinto, B. M. *J. Org. Chem.* **2000**, *65*, 220–226.
19. (a) Alabugin, I. V. *J. Org. Chem.* **2000**, *65*, 3910–3919; (b) Alabugin, I. V.; Manoharan, M.; Zeidan, T. A. *J. Am. Chem. Soc.* **2003**, *125*, 14014–14031.
20. Freeman, F.; Cha, C. *J. Phys. Org. Chem.* **2004**, *17*, 32–41.
21. Kleinpeter, E.; Koch, A.; Pihlaja, K. *Tetrahedron* **2005**, *61*, 7349–7358.
22. Cuevas, G.; Martínez-Mayorga, K.; Fernández-Alonso, M. C.; Jiménez-Barbero, J.; Perrin, C. L.; Juaristi, E.; López-Mora, N. *Angew. Chem., Int. Ed.* **2005**, *44*, 2360–2364.
23. Shainyan, B. A.; Ushakov, I. A.; Suslova, E. N. *J. Sulf. Chem.* **2006**, *27*, 3–13.
24. Wedel, T.; Müller, M.; Podlech, J.; Goesmann, H.; Feldmann, C. *Chem.—Eur. J.* **2007**, *13*, 4273–4281.

25. Frisch, M. J.; Trucks, G. W.; Schlegel, H. B.; Scuseria, G. E.; Robb, M. A.; Cheeseman, J. R.; Montgomery, J. A., Jr.; Vreven, T.; Kudin, K. N.; Burant, J. C.; Millam, J. M.; Iyengar, S. S.; Tomasi, J.; Barone, V.; Mennucci, B.; Cossi, M.; Scalmani, G.; Rega, N.; Petersson, G. A.; Nakatsuji, H.; Hada, M.; Ehara, M.; Toyota, K.; Fukuda, R.; Hasegawa, J.; Ishida, M.; Nakajima, T.; Honda, Y.; Kitao, O.; Nakai, H.; Klene, M.; Li, X.; Knox, J. E.; Hratchian, H. P.; Cross, J. B.; Bakken, V.; Adamo, C.; Jaramillo, J.; Gomperts, R.; Stratmann, R. E.; Yazyev, O.; Austin, A. J.; Cammi, R.; Pomelli, C.; Ochterski, J. W.; Ayala, P. Y.; Morokuma, K.; Voth, G. A.; Salvador, P.; Dannenberg, J. J.; Zakrzewski, V. G.; Dapprich, S.; Daniels, A. D.; Strain, M. C.; Farkas, O.; Malick, D. K.; Rabuck, A. D.; Raghavachari, K.; Foresman, J. B.; Ortiz, J. V.; Cui, Q.; Baboul, A. G.; Clifford, S.; Cioslowski, J.; Stefanov, B. B.; Liu, G.; Liashenko, A.; Piskorz, P.; Komaromi, I.; Martin, R. L.; Fox, D. J.; Keith, T.; Al-Laham, M. A.; Peng, C. Y.; Nanayakkara, A.; Challacombe, M.; Gill, P. M. W.; Johnson, B.; Chen, W.; Wong, M. W.; Gonzalez, C.; Pople, J. A. *Gaussian 03, revision B.03*; Gaussian: Pittsburg, PA, CT, 2003.
26. Ditchfield, R. *J. Chem. Phys.* **1972**, *56*, 5688–5691.
27. Wolinski, K.; Hinton, J. F.; Pulay, P. *J. Am. Chem. Soc.* **1990**, *112*, 8251–8260.
28. (a) Weinhold, F.; Landis, C. R. *Valency and Bonding: A Natural Bond Orbital Donor–Acceptor Perspective*; Cambridge University Press: Cambridge, 2005; (b) Glendening, E. D.; Reed, A. E.; Carpenter, J. E.; Weinhold, F. *NBO Version 3.1*; Gaussian: Pittsburgh, PA, CT, 2003.